Pis'ma v ZhETF, vol. 98, iss. 7, pp. 448 – 451

Electronic and magnetic properties of new 2D diluted magnetic semiconductor $La_{1-x}Ba_xZn_{1-x}Mn_xAsO$ from first-principles calculations

V. V. Bannikov, A. L. Ivanovskii[1)]

Institute of Solid State Chemistry, UB of the RAS, 620990 Ekaterinburg, Russia

Submitted 12 August 2013

Very recently, on the example of hole- and spin-doped semiconductor LaZnAsO, quite an unexpected area of potential applications of quasi-two-dimensional 1111-like phases was proposed (C. Ding et al., PRB 88:041102R, 2013) – as a promising platform for searching for new diluted magnetic semiconductors (DMSs). In this Letter, by means of the first-principles calculations, we have examined in detail the electronic and magnetic properties of LaZnAsO alloyed with Ba and Mn. Our results demonstrate that Ba or Mn doping transforms the parent non-magnetic semiconductor LaZnAsO into non-magnetic metal or magnetic semiconductor, respectively. On the other hand, the joint effect of these dopants (i.e. co-doping Ba + Mn) leads to transition of $La_{0.89}Ba_{0.11}Zn_{0.89}Mn_{0.11}AsO$ into the state of *magnetic metal*, which is formed by alternately stacked semiconducting non-magnetic blocks [$La_{0.89}Ba_{0.11}O$] and metallic-like magnetic blocks [$Zn_{0.89}Mn_{0.11}As$].

DOI: 10.7868/S0370274X13190089

The quaternary 1111-like phases with a tetragonal layered structure of the ZrCuSiAs-type form a broad family of materials with a set of exciting physical properties, review [1]. Till now intensive research efforts have been focused on two main groups of such 1111-like phases. The first group includes metallic-like phases, which draw attention basically as parent systems in search for new superconductors, see [2–6]. The second group comprises semiconductors, which are viewed as transparent materials and interesting systems with "natural multiple quantum wells" [7–9].

On the other hand, these 1111-like systems show a high flexibility to a large variety of constituent elements. Therefore the doping strategy provides wide and diverse possibilities for tuning their basic physical properties and opens up fascinating ways to control the functionalities of these materials. So, it was predicted theoretically that by substitution of *magnetic* ions for *nonmagnetic* ions (i.e. by spin doping) in non-magnetic *semiconducting* ZrCuSiAs-like phases, a set of new *magnetic* materials (such as magnetic semiconductors, magnetic half-metals, magnetic gapless semi-metals [10, 11], or bipolar magnetic semiconductors [12]) may be designed.

Very recently, the first experimental evidence supporting the aforementioned theoretical hints was reported [13]. Namely, using semiconducting [14–17] 1111-like LaZnAsO as a parent phase, simultaneous hole (*via* hetero-valent substitutions $La^{3+} \rightarrow Ba^{2+}$) and spin (*via* isovalent substitutions $Zn^{2+} \rightarrow Mn^{2+}$) doping has been successfully achieved. As a result, a series of new diluted magnetic semiconductors (DMSs) $La_{1-x}Ba_xZn_{1-x}Mn_xAsO$ with $0 \leq x \leq 0.2$, which exhibit ferromagnetic order with Curie temperature up to 40 K, was prepared [13]. Note that DMSs attracted now much attention owing to their wide application prospects in spintronic devices, reviews [18–21]. Moreover, the authors [13] assume that the similarity of the crystal structures and matching of the lattices for the discovered DMSs and other related 1111-like phases (such as superconducting $LaFeAsO_{1-x}F_x$ [2–6] or antiferromagnetic LaMnAsO [22]) can be favorable for further designing of multilayer functional materials.

In this Letter, a first-principles study was performed in order to get an insight into the basic electronic and magnetic properties of the newly discovered DMSs $La_{1-x}Ba_xZn_{1-x}Mn_xAsO$.

Firstly, the electronic properties of LaZnAsO as a parent compound of new DMSs were studied. This phase adopts a tetragonal (space group $P4/nmm$, $Z = 2$) lattice of the ZrCuSiAs-like structural type. This structure can be schematically described as a stacking of quasi-two-dimensional blocks [La_2O_2] and [Zn_2As_2] in the sequence $\ldots[La_2O_2]/[Zn_2As_2]/[La_2O_2]/[Zn_2As_2]\ldots$ The atomic positions are La: $2c$ $(1/4, 1/4, z_{La})$; Zn: $2b$ $(3/2, 1/4, 1/2)$; As: $2c$ $(1/4, 1/4, z_{As})$; and O: $2a$ $(3/4, 1/4, 0)$, where z_{La} and z_{As} are the so-called internal coordinates [23].

To understand the formation of the electronic and magnetic properties of the examined DMSs

[1)] e-mail: ivanovskii@ihim.uran.ru

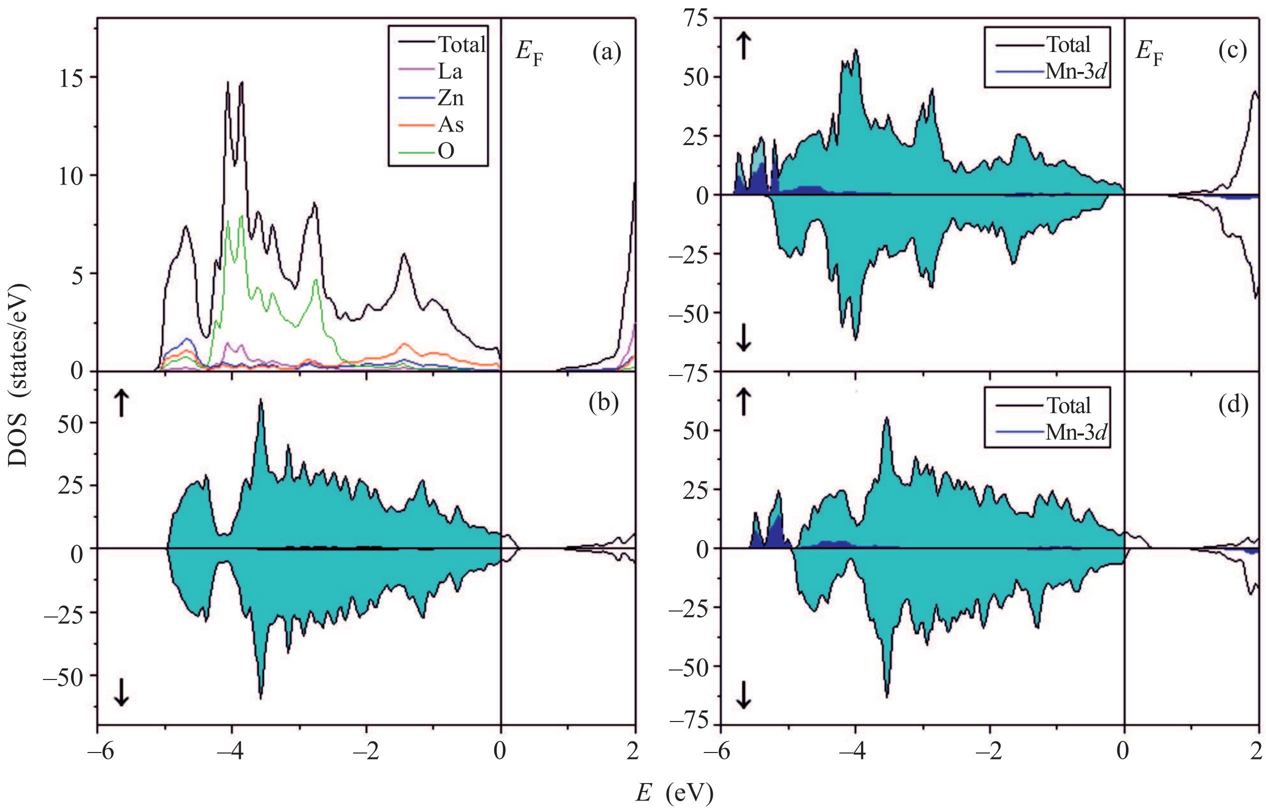

Fig. 1. Total and atomic-projected densities of states for: LaZnAsO (a); $La_{0.89}Ba_{0.11}ZnAsO$ (b); $LaZn_{0.89}Mn_{0.11}AsO$ (c), and $La_{0.89}Ba_{0.11}Zn_{0.89}Mn_{0.11}AsO$ (d). The partial Mn-$3d_{\uparrow,\downarrow}$ states also are shown in (c)–(d)

$La_{1-x}Ba_xZn_{1-x}Mn_xAsO$, we began with the parent phase LaZnAsO, and then consistently the doping effects of Ba (inside the [LaO] blocks) and of Mn (inside the [ZnAs] blocks) were examined, and finally, the co-doping effect (simultaneous substitutions $La^{3+} \to Ba^{2+}$ and $Zn^{2+} \to Mn^{2+}$) was simulated. For this purpose, the 72-atomic $3 \times 3 \times 1$ supercells were used, i.e. the nominal compositions of doped systems, namely $La_{0.89}Ba_{0.11}ZnAsO$, $LaZn_{0.89}Mn_{0.11}AsO$, and $La_{0.89}Ba_{0.11}Zn_{0.89}Mn_{0.11}AsO$ were studied. The impurities (Ba^{2+} and Mn^{2+} ions) were placed at the maximal distances from each other (in supercells) to exclude their interaction. Besides, for the Mn-containing systems, we considered the magnetic state in the assumption of ferromagnetic spin configuration.

The calculations were carried out by means of the full-potential method with mixed basis APW+lo (FLAPW) implemented in the WIEN2k suite of programs [24]. The plane-wave expansion was taken up to $R_{MT} \times K_{MAX}$ equal to 7, and the k sampling with $6 \times 6 \times 8$ k-points in the Brillouin zone was used. La($4f^0 5s^2 5p^6 5d^1 6s^2$), Zn($3d^{10} 4s^2 4p^0$), Mn($3d^5 4s^2 4p^0$), Ba($6s^2 6p^0 5d^0$), O($2s^2 2p^4$), and As ($4p^3 4s^2$) configurations were treated as valence states. To take the d-electron correlation into account, we included the on-site Coulomb interaction U in the GGA + U approach [25] as implemented in the WIEN2k code using the well-established Coulomb repulsion parameter $U = 6.9$ eV and Hund's parameter $J = 0.86$ eV [26].

In Fig. 1 the total and atomic projected densities of states (DOSs) for the parent phase LaZnAsO (as obtained for optimized lattice constants: $a = 4.0908$ Å and $c = 9.1495$ Å, and internal atomic coordinates: $z_{La} = 0.1341$ and $z_{As} = 0.6698$) are depicted. This system is a non-magnetic semiconductor (direct transitions in Γ point) with a calculated band gap (BG) at about 0.65 eV. This value is in reasonable agreement with the previously reported theoretical estimations (0.53 eV [17]), but is smaller than the experimental data (~ 1.5 eV [14, 16]) owing to the well-known underestimation of the BG values within the DFT based calculation methods. The near-Fermi region of LaZnAsO is composed predominantly of the states of blocks [ZnAs], whereas the states of blocks [LaO] are placed mainly in the interval 2–5 eV below E_F, see also [15, 17].

The hole doping of LaZnAsO (*via* hetero-valent substitutions $La^{3+} \to Ba^{2+}$) leads to partial emptying of the near-Fermi states, Fig. 1. As a result, $La_{0.89}Ba_{0.11}ZnAsO$ will behave as a *non-magnetic metal* with a non-zero density of states at the Fermi level ($N(E_F) = 0.524$ states/eV per one $La_{0.89}Ba_{0.11}ZnAsO$ form. unit). It is also noteworthy that the contributions from the states of Ba to the valence bands of $La_{0.89}Ba_{0.11}ZnAsO$ are negligible, i.e. these impurity atoms are in the form of cations Ba^{2+}.

Quite a different situation was observed for spin-doped LaZnAsO (*via* isovalent substitutions $Zn^{2+} \to \to Mn^{2+}$), see Fig. 1. According to our calculations, for $LaZn_{0.89}Mn_{0.11}AsO$ the Mn-3*d* states undergo essential spin splitting resulting in the formation of considerable local magnetic moments MM(Mn) $\sim 4.22\mu_B$. The Mn-$3d_\uparrow$ sub-band is filled and lies at the bottom of the valence band ($\sim$4–6 eV below E_F), while the Mn-$3d_\downarrow$ sub-band appears to be practically unoccupied and lies in the conductivity band (higher 1.5 eV above E_F). Taking into account both the calculated MM(Mn) and the character of Mn-$3d_{\uparrow,\downarrow}$ bands filling it may be assumed that Mn ions in $LaZn_{0.89}Mn_{0.11}AsO$ adopt an electronic configuration $3d^5$ and are present in the high-spin $^6A_1$ state (the discrepancy between the calculated MM(Mn) value and the theoretical one $2S\mu_B = 5\mu_B$ can be attributed to computational MT-spheres formalism always providing a lower-bound estimation of the atomic magnetic moment).

On the other hand, the Mn-3*d* states do not contribute to the near-Fermi region, and $LaZn_{0.89}Mn_{0.11}AsO$ behaves as a *magnetic semiconductor*, which is characterized by two gaps: $\Delta_\uparrow \approx 0.70$ eV and $\Delta_\downarrow = 0.82$ eV. Thus, only manganese implanted into LaZnAsO provides no additional carriers in the doped system, which remains semiconducting [13].

The joint effect of the aforementioned impurities (Ba and Mn) leads for $La_{0.89}Ba_{0.11}Zn_{0.89}Mn_{0.11}AsO$ (Fig. 1) to partial emptying of the valence band (due to the holes provided by Ba impurities) and to magnetization – due to spin splitting of Mn-3*d* states similar to that in $LaZn_{0.89}Mn_{0.11}AsO$. The calculated magnetic moments MM(Mn) are $4.20\mu_B$ – quite close to that obtained for $LaZn_{0.89}Mn_{0.11}AsO$ supporting the supposition about Mn ions states to be the same. Note that additional small antiferromagnetically ordered magnetic moments (of $\sim 0.03\mu_B$) are induced at the first neighboring As sites, whereas magnetization for other atoms of the $La_{0.89}Ba_{0.11}Zn_{0.89}Mn_{0.11}AsO$ phase is absent. Thus, the magnetization of $La_{0.89}Ba_{0.11}Zn_{0.89}Mn_{0.11}AsO$ arises exclusively inside blocks [Zn(Mn)As], whereas the adjacent blocks [La(Ba)O] retain their non-magnetic character.

This situation is illustrated in Fig. 2, where the total and atomic-projected states of the examined

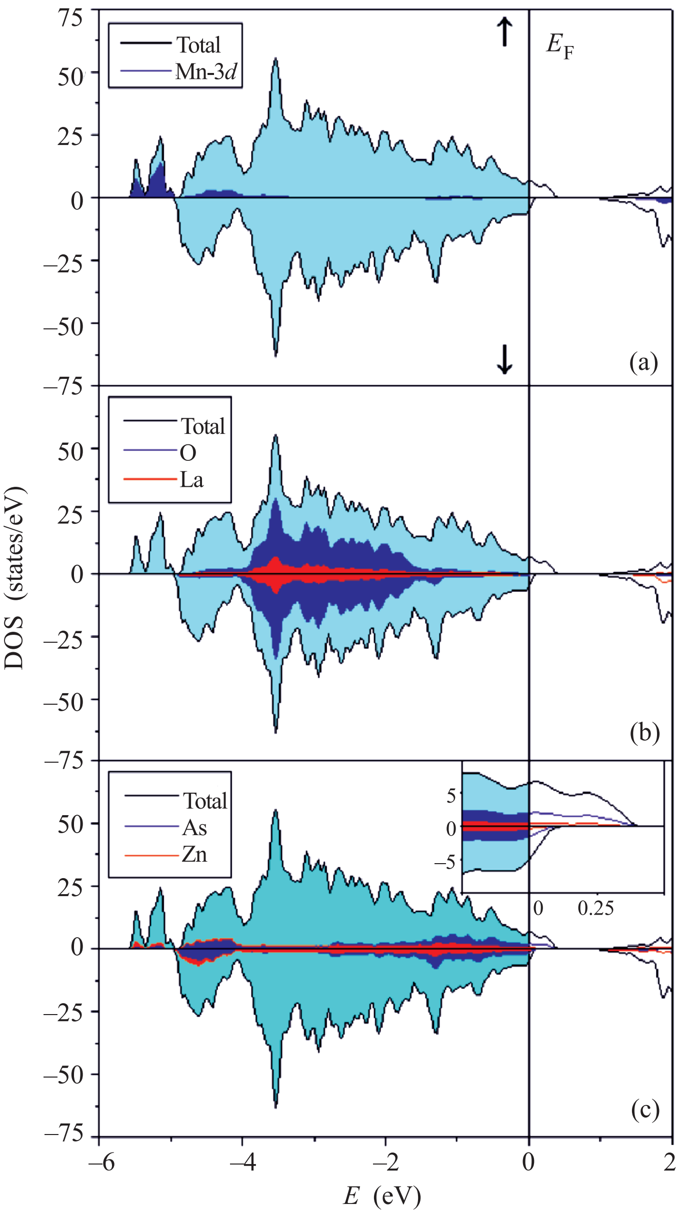

Fig. 2. Total and spin- and atomic-projected densities of states of co-doped $La_{0.89}Ba_{0.11}Zn_{0.89}Mn_{0.11}AsO$. The partial As and Zn states in the near-Fermi region are shown in the inset

$La_{0.89}Ba_{0.11}Zn_{0.89}Mn_{0.11}AsO$ are depicted. We can see that the states of blocks $[La_{0.89}Ba_{0.11}O]$ are placed below the Fermi level and retain their non-magnetic character, whereas the density of states at the Fermi level ($N_\uparrow(E_F) = 0.393$ and $N_\downarrow(E_F) = 0.243$ states/eV per form. unit) is formed mainly by the Zn and As states of blocks $[Zn_{0.89}Mn_{0.11}As]$, which contain also magnetic centers. Thus, our results reveal that generally

$La_{0.89}Ba_{0.11}Zn_{0.89}Mn_{0.11}AsO$ can be characterized as a *magnetic metal*, which is formed by alternately stacked semiconducting non-magnetic blocks $[La_{0.89}Ba_{0.11}O]$ and metallic-like magnetic blocks $[Zn_{0.89}Mn_{0.11}As]$.

In summary, using the $GGA+U$ approach, we have analyzed the electronic and magnetic properties of the recently synthesized $LaZn_{1-x}Mn_xAsO$ and $La_{1-x}Ba_xZn_{1-x}Mn_xAsO$ systems at $x = 0.11$. In both compounds, Mn ions obtain considerable local magnetic moments and are in the high-spin ground state. However, $LaZn_{0.89}Mn_{0.11}AsO$ remains to be a semiconductor, while hole-doped $La_{0.89}Ba_{0.11}Zn_{0.89}Mn_{0.11}AsO$ should be conductive at $T = 0$ K. This result qualitatively agrees with the suppositions of the authors [13] about the RKKY-like type of interactions between Mn magnetic centers in LaZnAsO. Actually, realization of RKKY-like interactions requires some amount of carriers to be present. According to the experiment [13], $LaZn_{0.89}Mn_{0.11}AsO$, predicted as a semiconductor, is paramagnetic at $T = (2-200)$ K, because the small concentration of thermally provided carriers is not enough to stabilize the Mn–Mn exchange interactions. The codoped $La_{0.89}Ba_{0.11}Zn_{0.89}Mn_{0.11}AsO$ possesses hole carriers at $T = 0$ K and exhibits bulk magnetization at T below 40 K [13], possibly stabilized by carriers-mediated exchange. At the same time, the maximal experimental value of magnetization per Mn atom is significantly smaller than the theoretically one ($0.7\mu_B$ *vs* $4.2\mu_B$ for $x \sim 0.1$). This may be related to the oscillating dependence of the RKKY interaction sign on the distance between centers and to the disordered distribution of impurity Mn atoms in the synthesized bulk samples.

The authors acknowledge the support from the RFBR (grant # 11-03-00052-a).

1. R. Pöttgen and D. Johrendt, Z. Naturforsch. b **63**, 1135 (2008).
2. M. V. Sadovskii, Physics – Uspekhi **51**, 1201 (2008).
3. A. L. Ivanovskii, Physics – Uspekhi **51**, 1229 (2008).
4. Z. A. Ren and Z. X. Zhao, Adv. Mater. **21**, 4584 (2009).
5. J. A. Wilson, J. Phys. Condens. Matter **22**, 203201 (2010).
6. D. C. Johnson, Adv. Phys. **59**, 803 (2010).
7. K. Ueda, H. Hiramatsu, H. Ohta et al., Phys. Rev. B **69**, 55305 (2004).
8. K. Ueda, H. Hiramatsu, T. Kamiya, and H. Hosono, Thin Solid Films **496**, 8 (2006).
9. H. Hiramatsu, T. Kamiya, M. Hirano, and H. Hosono, Physica C **469**, 657 (2009).
10. V. V. Bannikov, I. R. Shein, and A. L. Ivanovskii, Solid State Commun. **150**, 2069 (2010).
11. V. V. Bannikov and A. L. Ivanovskii, Phys. Solid State **54**, 1117 (2012).
12. V. V. Bannikov and A. L. Ivanovskii, JETP Lett. **96**, 735 (2013).
13. C. Ding, H. Man, Ch. Qin et al., Phys. Rev. B **88**, 041102R (2013).
14. K. Kayanuma, R. Kawamura, H. Hiramatsu et al., Thin Solid Films **516**, 5800 (2008).
15. V. V. Bannikov, I. R. Shein, and A. L. Ivanovskii, Mater. Chem. Phys. **116**, 129 (2009).
16. H. Lincke, R. Glaum, V. Dittrich et al., Ztsch. Anorgan. Allgem. Chem. **635**, 936 (2009).
17. L. Zhang and D. J. Singh, Phys. Rev. B **80**, 214530 (2009).
18. I. Zutic, J. Fabian, and S. Das Sarma, Rev. Mod. Phys. **76**, 323 (2004).
19. H. Katayama-Yoshida, K. Sato, T. Fukushima et al., Phys. Stat. Sol. a **204**, 15 (2007).
20. A. L. Ivanovskii, Physics – Uspekhi **50**, 1031 (2007).
21. T. Dietl, Nature Mater. **9**, 965 (2010).
22. N. Emery, E. J. Wildman, J. M. S. Skakle, and A. C. Mclaughlin, Phys. Rev. B **83**, 144429 (2011).
23. Y. Takano, S. Komaatsuzaki, H. Komasaki et al., J. Alloys Compd. **451**, 467 (2008).
24. P. Blaha, K. Schwarz, G. Madsen et al., WIEN2k, *An Augmented Plane Wave Plus Local Orbitals Program for Calculating Crystal Properties, Vienna University of Technology*, Vienna, 2001.
25. M. T. Czyzyk and G. A. Sawatzky, Phys. Rev. B **49**, 14211 (1994).
26. V. I. Anisimov, J. Zaanen, and O. K. Andersen, Phys. Rev. B **44**, 943 (1991).